

Statistics of Coulomb Blockade Peak Spacings

S. R. Patel, S. M. Cronenwett, D. R. Stewart, A. G. Huibers, and C. M. Marcus
Department of Physics, Stanford University, Stanford, CA 94305

C. I. Duruöz and J. S. Harris
Electrical Engineering Department, Stanford University, Stanford, CA 94305

K. Campman and A. C. Gossard
*Materials Department, University of California at Santa Barbara
Santa Barbara, CA 93106*

PACS #: 73.23Hk, 73.20Dx, 05.45+b

(submitted PRL: 8/4/97)

Distributions of Coulomb blockade peak spacing are reported for large ensembles of both unbroken (magnetic field $B = 0$) and broken ($B \neq 0$) time reversal symmetry in GaAs quantum dots. Both distributions are symmetric and roughly gaussian with a width $\sim 2\text{--}6\%$ of the average spacing, with broad, non-gaussian tails. The distribution is systematically wider at $B = 0$ by a factor of $\sim 1.2 \pm 0.1$. No even-odd spacing correlations or bimodal structure in the spacing distribution is found, suggesting an absence of spin-degeneracy. There is no observed correlation between spacing and peak height.

For some time it has been appreciated that electron transport in mesoscopic systems exhibits quantum interference effects with universal statistical features, and that this universality can be associated with the underlying universality of quantum chaos [1] and its mathematical description in terms of random matrix theory (RMT) [2, 3]. This approach has been quite successful in describing low-temperature transport in open quantum systems (i.e. systems with large conductance, $g > e^2/h$, to reservoirs) where a single-particle picture apparently provides an adequate description of the physics. Recent application of RMT to ground state properties of nearly isolated quantum dots—in particular, in characterizing the distributions of Coulomb blockade (CB) conductance peak heights [4]—has also been remarkably successful [5, 6].

On the other hand, experiments by Sivan *et al.* [7] and Simmel *et al.* [8] indicate that the most basic prediction of RMT, namely the famous Wigner surmise for the distribution of level spacings, fails to describe the fluctuations of Coulomb blockade peak spacing, suggesting that fluctuations in the energy separation between adjacent ground states of a quantum dot—the so-called addition spectrum—appear not to be distributed according to RMT. The failure of RMT in this case is perhaps not surprising, since this theory was not intended to describe ground state properties, even in systems with single-particle-like excitations above the ground state. Unfortunately, this failure leaves no theory that can adequately characterize (even statistically) the ground state addition spectrum of degenerate confined Fermi systems.

In this Letter, we present an extensive study of the distributions of ground state energy spacings as measured from the spacings of CB peaks in GaAs quantum dots, in both zero and non-zero magnetic field, including over 20,000 CB peaks measured in seven devices. Consistent with previous experiments [7, 8], we find that the distribution of CB peak spacings are not qualitatively described by single-particle RMT. In contrast to these experiments, however, we find that the width of the distribution of fluctuations is rather narrow, comparable (once scaled) to the single particle level spacing, and shows the effects

of time reversal symmetry breaking comparable to RMT predictions, suggesting that quantum effects play some role in determining the distributions. The extensive data set allows full distributions of peak spacing fluctuations to be measured accurately for the first time. What is found is that both $B = 0$ and $B \neq 0$ distributions are roughly gaussian, with significantly wider than gaussian tails. We also find no correlation between peak height properties (reflecting eigenfunction properties) and peak spacings (reflecting eigenvalue properties).

Ground state energy fluctuations are measured using the Coulomb blockade of conductance, which appears in quantum dots with tunneling leads (lead conductance $g_l, g_r < 2e^2/h$) whenever the temperature T and source-drain voltage V_{sd} are less than the charging energy $E_C = e^2/C_{dot}$, where C_{dot} is the total capacitance of the dot [9-11]. In this regime, dot conductance is suppressed except when the N and $(N+1)$ -electron ground state energies of the dot are degenerate. The dot potential can be tuned through these degeneracies by varying the voltage V_g applied to a nearby metallic gate, producing a series of thermally broadened peaks in conductance which are nearly periodic in V_g .

At low temperature and bias, $(k_B T, eV_{sd}) < \Delta$ (where $\Delta = 2\pi\hbar^2/m^*A$ is the average single particle level spacing for *spin-degenerate* levels, m^* is the electron effective mass, and A is the dot area), transport on a CB peak is a resonant process, making the degeneracy condition and hence the peak location sensitive to the discrete level spectrum of the dot. A simple and often assumed model connecting level spacing statistics and CB peak spacing is the so-called ‘constant interaction’ (CI) model, in which the separation between ground state energies of the dot probed by CB is separated into two parts, a charging energy E_C that is independent of (or at most slowly varying with) the number of electrons on the dot, N , and a fluctuating part associated with a discrete quantum level spacing. This separation assumes that fluctuations in E_C due to charge rearrangement in the ground state upon

adding an electron are small compared to Δ . Within the CI model, the spacing (in gate voltage) between CB peaks, $\Delta V_g^i = V_g^{i+1} - V_g^i$, where V_g^i is the center position of the i^{th} peak, is given by

$$e\eta \Delta V_g^i = \begin{cases} (\varepsilon^{i+1} - \varepsilon^i) + E_c & (i \text{ even}) \\ E_c & (i \text{ odd}) \end{cases} \quad (1)$$

where ε^i is the i^{th} single-particle energy level and $\eta = C_g / C_{dot}$ is the ratio of gate capacitance to total dot capacitance, the ‘lever arm’ which converts gate voltage to dot energy, also assumed to vary slowly with i . The dependence of Eq. 1 on whether i is even or odd reflects the assumed spin degeneracy of levels in the CI model.

Now, if one further assumes that level spacings $(\varepsilon^{i+1} - \varepsilon^i)$ are distributed according to RMT statistics then the distribution $P(v)$ of normalized fluctuations in peak spacing $v = (\Delta V_g^i - \langle \Delta V_g^i \rangle) / \langle \Delta V_g^i \rangle$ will consist of a δ function for the case of i odd plus a Wigner-Dyson distribution ($\propto v e^{(-\pi v^2/4)}$ for $B = 0$ and $\propto v^2 e^{(-4v^2/\pi)}$ for $B \neq 0$) for the case i even, up to a horizontal shift to center $P(v)$ at zero. The brackets $\langle \cdot \rangle$ denote an average over an ensemble of levels. Note that within RMT, the width (i.e. standard deviation), σ , of $P(v)$ depends on time-reversal symmetry; for $\Delta \ll E_c$, CI+RMT gives $\sigma = 0.52(0.42)\Delta/E_c$ for $B = 0$ ($B \neq 0$). The ratio $\sigma_{B=0}/\sigma_{B \neq 0} \sim 1.2$ follows from CI+RMT for any Δ/E_c . For GaAs dots of the type described here and in Ref. [7, 8], one expects roughly $\sigma \sim 0.03$, depending slightly on the dot shape and size, based on experimental values of Δ and E_c (see Table 1). Previous experiments [7, 8] found CB peak spacing fluctuations considerably larger than this value, of order 0.1–0.15 of the average spacing. The large fluctuations found in the experiment as well as supporting numerics lead Sivan *et al.* [7] to

suggest that *classical* charging energy fluctuations proportional to E_C not included in the CI+RMT model dominate peak spacing fluctuations. Recent Hartree-Fock calculations suggest that such fluctuations due to charge rearrangement should be small compared to Δ [12]. In the present study, we find values of σ that are consistent in size and magnitude of symmetry-breaking effect with the CI+RMT predictions, but (as with Refs. [7, 8]) we find a unimodal, roughly symmetric $P(v)$ that is inconsistent with CI+RMT.

The quantum dots we have measured are formed by gate depletion of a two-dimensional electron gas (2DEG) in a GaAs/AlGaAs heterostructure (see Table 1 for device parameters). All dot dimensions were smaller than the bulk mean free path so that transport within the dots is ballistic. The irregular dot shapes were designed to produce chaotic scattering while multiple gates allowed ensemble averaging using shape distortion. Charging energies are measured from the relation $E_C \sim e\eta \langle \Delta V_g \rangle$, based on Eq. 1 with $\Delta \ll E_C$, with the ‘lever arm’ $\eta = C_g/C_{dot}$ extracted from the temperature dependence of the peak width [10]. All measurements were made in a dilution refrigerator at base temperature (30 mK) using two-wire ac lockin techniques with a voltage bias of 5 μ V at 11 Hz. The electron temperature, determined by fitting peak width versus temperature [10], was ~ 100 mK for all devices. Ensemble statistics were collected by sweeping one gate voltage, V_{g1} , over ~ 20 peaks then incrementing magnetic field or a second gate voltage, V_{g2} , to yield a new ensemble of peaks. While the heights of nearby CB peaks show considerable correlation (Fig. 1a), peak spacings appear uncorrelated (Fig. 1b, 1c). We estimate the number of “independent” peak spacings, n_i in Table 1, as the number of peaks measured in each scan of V_{g1} multiplied by the number of scans over independent peaks based on height. All peak spacing data are based on relatively small CB peaks, in the range 0.01 to 0.1 e^2/h . For this range of heights, the valleys between peaks have zero conductance within the noise of the measurement.

A typical set of CB peaks is shown in Fig. 1a. To extract peak spacing, each peak is fit by a \cosh^2 form [10] and spacing is determined from the centers of the fits (Fig. 1b). The decreasing average spacing as V_{g1} increases (i.e. as electrons are added to the dot), reflects an increasing C_{dot} with increasing N . A running average spacing $\langle \Delta V_{g1}^i \rangle$ is found from the best fit line (dashed in Fig. 1b) and used to define the normalized fluctuations, $\nu = (\Delta V_g^i - \langle \Delta V_g^i \rangle) / \langle \Delta V_g^i \rangle$, shown in Fig. 1c. Combined histograms of peak spacings of ~ 2300 independent peaks ($\sim 10^4$ total peaks) from three dots with similar device parameters (dots 3, 4, and 5) are shown in Fig. 2. Both the $B = 0$ and $B \neq 0$ histograms are roughly symmetric and gaussian. A gaussian fit to the $B = 0$ histogram gives a standard deviation $\sigma_{B=0}(\nu)_f = 0.019$ (the subscript f indicates ‘gaussian fit’) whereas a direct evaluation of the second moment of the spacing data set yields $\sigma_{B=0}(\nu) = 0.027$. This difference results from broad non-gaussian tails, which are clearly seen in a logarithmic plot (insets, Fig. 2). The $B \neq 0$ distribution width from a gaussian fit of the histogram yields $\sigma_{B \neq 0}(\nu)_f = 0.015$ and the second moment of the data gives $\sigma_{B \neq 0}(\nu) = 0.022$. By either method, a ratio $\sigma_{B=0} / \sigma_{B \neq 0} \sim 1.2\text{--}1.3$ is obtained. Widths for other devices are given in Table 1. For all devices $\sigma_{B=0} / \sigma_{B \neq 0} \sim 1.1\text{--}1.3$, consistent with CI+RMT. However, since $P(\nu)$ is not Wigner-Dyson distributed (with or without the δ -function) the precise agreement of the ratio $\sigma_{B=0} / \sigma_{B \neq 0}$ may be coincidental. The temperature dependence of $\sigma_{B \neq 0}(\nu)$ from device 1 is shown in inset Fig. 2b for two different dot configurations ($\Delta = 42 \mu eV$ and $\Delta = 29 \mu eV$) corresponding to different applied gate voltages. Measurements in the smaller dot configuration indicate that $\sigma_{B \neq 0}(\nu)$ saturates to a value ($\sigma \sim 0.02$ at $k_B T / \Delta \sim 0.2$) which is considerably smaller than in previous studies.

We next investigate correlations between peak spacing fluctuations and peak height fluctuations [5, 6]. Within RMT, no correlations are expected since height fluctuations depend on eigenfunctions [4] while spacings fluctuations depend on eigenvalues;

eigenfunctions and eigenvalues are uncorrelated within RMT [13]. Figure 3 shows CB peaks and spacings for $B \neq 0$ (for device 4) as gray-scale plots over gate voltages V_{g1} and V_{g2} . Stripes of roughly constant height moving downward to the right in Fig. 3a indicate that effectively the same CB peak is being measured many times as V_{g1} is increased and V_{g2} is decreased (on the voltage scale of the CB spacing, the effects of shape distortion are small). Spacing fluctuations for the same data set show similar striped structure (Fig. 3b) as expected if, again, it is roughly the same peak spacing being measured for different combinations of V_{g1} and V_{g2} . The stripes in Fig. 3b indicate that the spacing measurement is not noise limited, since peak spacings follow same lines as peak heights. The plot also shows that spacing fluctuations are not correlated within a row, i.e. neighboring spacings are not correlated. This contrasts the peak heights, which are correlated over 3–7 peaks (depending on the device) within a row [5]. We find that the spacing ν between adjacent peaks ($i+1$ and i) is not correlated with either the normalized height difference of the two peaks $\Delta\tilde{g} = (g_{\max}^{i+1} - g_{\max}^i)/\langle g_{\max} \rangle$ or their normalized average height, $\tilde{g} = (g_{\max}^{i+1} + g_{\max}^i)/2\langle g_{\max} \rangle$, as shown in Fig. 3c and 3d.

In summary, we have measured Coulomb blockade peak spacing fluctuations for very large ensembles at both $B = 0$ and $B \neq 0$ in GaAs quantum dots. We find roughly gaussian distributions with wide tails and widths ~ 0.02 – 0.06 times the average peak spacing ($\sim E_C$), smaller by factor of 3–5 than measured previously [7, 8]. The widths we observe are consistent with the CI+RMT model, as is the ratio $\sim 1.2 \pm 0.1$ of widths for $B = 0$ and $B \neq 0$. The absence of a bimodal distribution or any even-odd structure in the spacings suggests an unexpected absence of spin degeneracy. Finally, we observe no correlation between peak spacing fluctuations and average peak height or peak height differences.

We thank J. A. Folk and D. Sprinzak for assistance with the measurements. Also, we thank O. Agam, I. Aleiner, B. Altshuler, and U. Sivan for valuable discussions. Work at Stanford supported in part by the Army Research Office, the Office of Naval Research YIP program, the NSF-NYI and PECASE programs, the A. P. Sloan Foundation, JSEP, and the Hertz Foundation (A.G.H.). Work at UCSB supported by AFOSR and QUEST.

References

1. B. L. Altshuler and B. D. Simons, in *Mesoscopic Quantum Physics*, edited by E. Akkermans, G. Montambaux, J.-L. Pichard, and J. Zinn-Justin (Elsevier, Amsterdam, 1995).
2. C. W. J. Beenakker, Rev. Mod. Phys. **69**, 731 (1997).
3. T. Guhr, A. Mueller-Groeling, and H. A. Weidenmueller, cond-mat/9707301, (1997); M. C. Gutzwiller, *Chaos in Classical and Quantum Mechanics* (Springer-Verlag, New York, 1990).
4. R. A. Jalabert, A. D. Stone, and Y. Alhassid, Phys. Rev. Lett. **68**, 3468 (1992).
5. J. A. Folk *et al.*, Phys. Rev. Lett. **76**, 1699 (1996).
6. A. M. Chang *et al.*, Phys. Rev. Lett. **76**, 1695 (1996).
7. U. Sivan *et al.*, Phys. Rev. Lett. **77**, 1123 (1996).
8. F. Simmel, T. Heinzel, and D. A. Wharam, Europhys. Lett. **38**, 123 (1997).
9. D. V. Averin and K. K. Likharev, in *Mesoscopic Phenomena in Solids*, edited by B. L. Altshuler, P. A. Lee, and R. A. Webb (Elsevier, Amsterdam, 1991).
10. C. W. J. Beenakker, Phys. Rev. B **44**, 1646 (1991).
11. L. P. Kouwenhoven *et al.*, in *Proceedings of the NATO ASI Workshop*, edited by L. P. Kouwenhoven, L. L. Sohn, and G. Schön (Kluwer Academic Publishers, Dordrecht, 1997).
12. Y. M. Blanter, A. D. Mirlin, and B. A. Muzykantskii, Phys. Rev. Lett. **78**, 2449 (1997).
13. T. A. Brody *et al.*, Rev. Mod. Phys. **53**, (1981).

Parameter	dot 1	dot 2	dot 3	dot 4	dot 5	dot 6	dot 7
A (μm^2)	0.17	0.20	0.32	0.34	0.38	0.47	0.50
d (\AA)	900	900	800	800	900	800	900
Δ (μeV)	42	36	22	21	19	15	14
E_C (μeV)	560	760	580	500	380	600	320
N	340	400	900	1000	800	1400	1000
n_i	190	70	140	830	1300	710	420
$\sigma_{B=0}(\nu)$ ($\times 10^{-3}$)	--	48 (7)	38 (2)	25 (2)	25 (3)	43 (2)	56 (3)
$\sigma_{B \neq 0}(\nu)$ ($\times 10^{-3}$)	18 (2)	34 (4)	23 (3)	22 (1)	20 (2)	38 (2)	43 (2)
$\frac{\sigma_{B=0}(\nu)}{\sigma_{B \neq 0}(\nu)}$	--	1.3 (0.2)	1.7 (0.2)	1.2 (0.1)	1.2 (0.2)	1.1 (0.1)	1.3 (0.1)

Table 1. Device parameters and measured spacing statistics at $T \sim 100$ mK: dot area (A), 2DEG depth (d), mean level spacing ($\Delta = 2\pi\hbar^2 / m^* A$), charging energy ($E_C = e^2 / C_{dot}$), number of electrons in dot (N), number of statistically independent peak spacings (n_i), and peak spacing distribution width at $B = 0$ ($\sigma_{B=0}(\nu)$) [$B \neq 0$ ($\sigma_{B \neq 0}(\nu)$)] with uncertainties in parentheses. Devices 1, 2, 5, and 7 (3, 4, and 6) have a sheet density $n_s \sim 2 \times 10^{11} \text{ cm}^{-2}$ ($3 \times 10^{11} \text{ cm}^{-2}$) and mobility $\mu \sim 1.4 \times 10^5 \text{ cm}^2 / \text{Vs}$ ($6.5 \times 10^5 \text{ cm}^2 / \text{Vs}$).

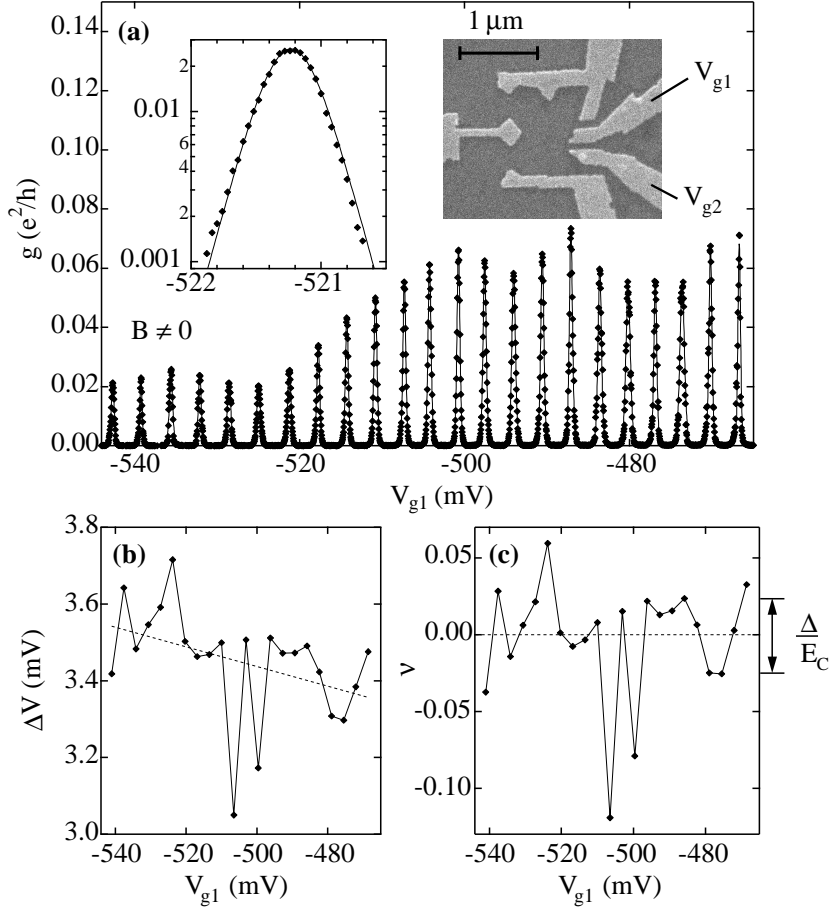


Fig. 1. (a) Coulomb blockade peaks (diamonds) as a function of gate voltage V_{g1} for device 7. Solid curve shows fit to \cosh^2 lineshape. Left inset: Detailed view of a peak on log-linear scale. Right inset: Micrograph of device 6, other devices are similar. (b) Peak spacings extracted from data in (a). Dashed line is best fit to data, corresponding to $\langle \Delta V_{g1}^i \rangle$. (c) Dimensionless peak spacing fluctuations ($\nu = (\Delta V_{g1}^i - \langle \Delta V_{g1}^i \rangle) / \langle \Delta V_{g1}^i \rangle$) as a function of gate voltage for data in (a,b). Normalized average level spacing Δ/E_C indicated on the right (See Table 1).

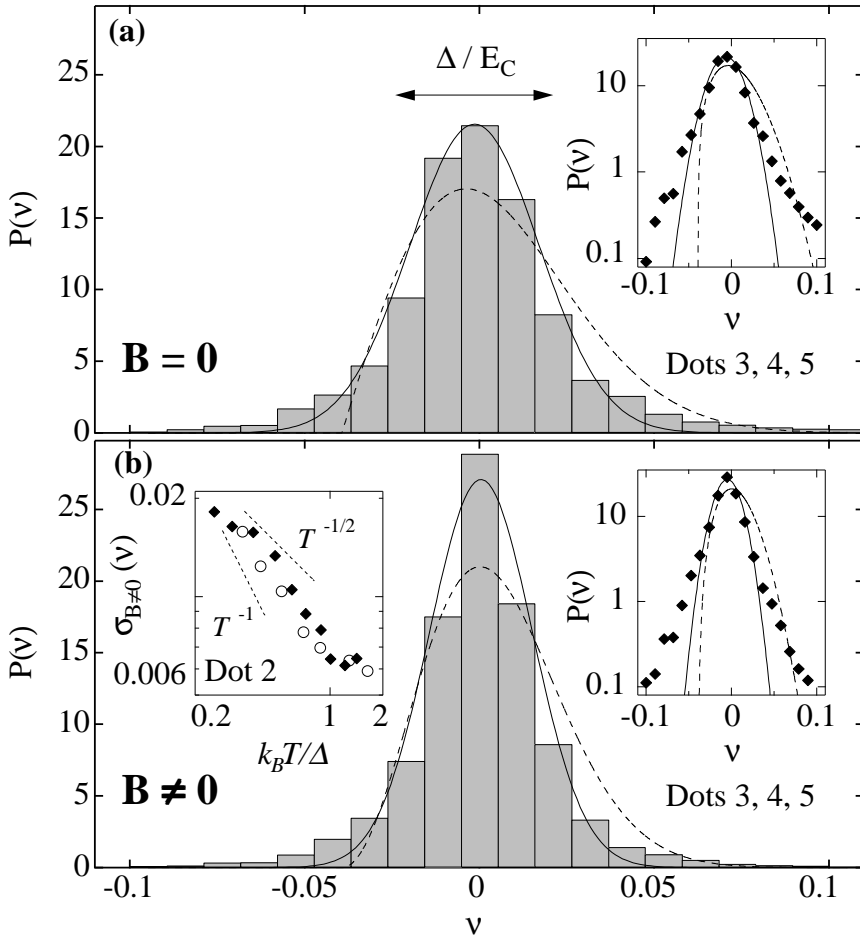


Fig. 2. Normalized peak spacing histogram (bars) for $B = 0$ (a) and $B \neq 0$ (b) for devices 3, 4, and 5. Solid line shows best fit to normalized gaussian of width 0.019 (0.015) for $B = 0$ ($B \neq 0$). Dashed line shows Wigner-Dyson distribution for Δ / E_C averaged over the 3 devices. The $B = 0$ histogram is wider by a factor of ~ 1.2 than the $B \neq 0$ histogram. Data represents 4,300 (10,800) peaks from the devices with ~ 720 (1600) statistically independent for $B = 0$ ($B \neq 0$). Horizontal arrow indicates mean level spacing. Right insets: Plots of histogram (diamonds) and best fit gaussian (solid line) on log-linear scale. Dashed lines are Wigner-Dyson distributions. (b) Left inset: Temperature dependence of $\sigma_{B \neq 0}(v)$ for device 1 on log-log scale with $\Delta = 42 \mu eV$ (solid diamonds) and $\Delta = 29 \mu eV$ (open circles); data saturates to noise floor above $k_B T \sim \Delta$. Solid diamonds show low-temperature saturation of $\sigma_{B \neq 0}(v)$; dashed lines show $T^{-1/2}$ and T^{-1} dependence for comparison.

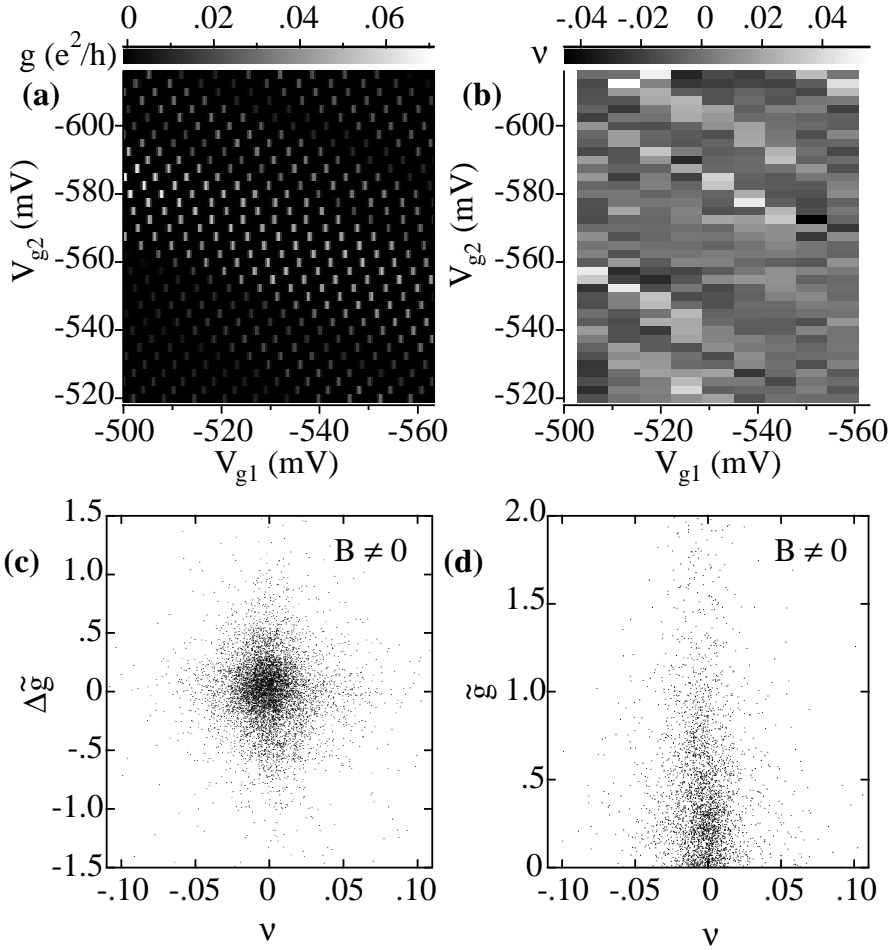


Fig. 3. (a) Two-dimensional grayscale plot of conductance (scale given by top horizontal bar) as a function of V_{g2} and V_{g1} for device 4 at $B = 60$ mT. Peaks follow lines of \sim constant conductance. (b) Density plot of peak spacing fluctuations v as a function of V_{g2} and approximate gate voltage V_{g1} for data displayed in (a); spacing fluctuations follow the same lines of slope as the peaks indicating parametric fluctuations of spacings. (c) Scatter plot of adjacent peak height differences $\Delta\tilde{g} = (g_{\max}^{i+1} - g_{\max}^i)/\langle g_{\max} \rangle$ and v consisting of all $B \neq 0$ data for dot 4. (d) Scatter plot of adjacent peak average height $\tilde{g} = (g_{\max}^{i+1} + g_{\max}^i)/2\langle g_{\max} \rangle$ as a function of v for the same data set as (c). Note that there are no observable correlations between v and peak height differences (c) or average peak height (d).